

## Effect of SnO<sub>2</sub> thickness variation on property of SnO<sub>2</sub>/Ag/Nb<sub>2</sub>O<sub>5</sub>/SiO<sub>2</sub>/SnO<sub>2</sub> multi layer film

Jin-Gyun Kim, Sang-Moo Yoo and Gun-Eik Jang\*

Department of Materials Engineering, Chungbuk National University, Cheongju 362-763, Korea

This study systematically investigates the dependence of the optical and electrical properties as a function of top SnO<sub>2</sub> thickness of SnO<sub>2</sub>/Ag/Nb<sub>2</sub>O<sub>5</sub>/SiO<sub>2</sub>/SnO<sub>2</sub> multi-layer films deposited on a glass substrate at room temperature. The results of an EMP simulation suggested that a multilayered thin film consisting of SnO<sub>2</sub> (45 nm)/Ag (10 nm)/Nb<sub>2</sub>O<sub>5</sub> (10 nm)/SiO<sub>2</sub> (10 nm)/SnO<sub>2</sub> (30 nm) exhibited a high transmittance of 88.8% at 550 nm while the experimentally-measured transmittance showed 85.3%, which was somewhat lower than what is shown with the simulation data. The lowest  $R_s$  and  $\rho$  value were of about 5.81  $\Omega$ /sq and 5.81  $\times 10^{-5} \Omega \cdot \text{cm}$ , and these were obtained with a multi-layered structure consisting of SnO<sub>2</sub> (40 nm)/Ag (10 nm)/Nb<sub>2</sub>O<sub>5</sub> (10 nm)/SiO<sub>2</sub> (10 nm)/SnO<sub>2</sub> (30 nm). However, the sheet resistance and resistivity of the SnO<sub>2</sub>/Ag/Nb<sub>2</sub>O<sub>5</sub>/SiO<sub>2</sub>/SnO<sub>2</sub> multi layer film increased systematically with an increase in the thickness of the SnO<sub>2</sub> layer from 40 to 55 nm. The  $\Phi_{TC}$  values of the SnO<sub>2</sub>/Ag/Nb<sub>2</sub>O<sub>5</sub>/SiO<sub>2</sub>/SnO<sub>2</sub> multi layer films were shown to be in the range from 10.3 to 33.5  $\times 10^{-3} \Omega^{-1}$ .

**Key words:** TMT structure, Transmittance, Sheet resistance,  $\Phi_{TC}$ .

### Introduction

Transparent conducting electrodes (TCEs) are important in a wide variety of applications, including in optoelectronics, photovoltaic devices and systems such as solar cells, organic light emitting diodes, and liquid crystal displays [1-2]. So far, research has been successfully conducted in the area of transparent conducting oxide (TCO) materials [3-8], and recently, insertion of ultrathin metal layer sandwiched between the two TCO layers has been studied to develop transparent TCEs. The TCO/metal/TCO (TMT) multi layer structures have been designed to achieve both a high conductivity and high transmittance in the visible range and have also shown a relatively better chemical stability than for a single-layered metal film [9-15].

Among many commercial applications, touch screens are becoming increasingly popular because of their ease and versatility of operation as well as their cost effectiveness. However, when the touch sensor panel in touch screens is used in a bright environment, the incident light can hit the interface between the layers of the stackup with mismatched refractive indices and can reflect off those interfaces. The light reflected from those interfaces can give rise to the appearance of fringes on the touch sensor panel, which can be visually distracting, and this problem poses one of the most critical issues for commercial applications.

In order to reduce the fringe effect, which is due to the reflectance change at the interface, an index matching layer with high and low refractive index materials can be placed between the metal and TCO as one of possible solutions using a TMT structure. In particular, the presence of the index matching layer is known to reduce the visibility of the drive lines and the sense lines in the touch sensor panel [16-17]. However, none of previous studies have been undertaken to study the modification of the optical properties through the addition of index matching layers into tri-layer structures.

In the present study, a hybrid film with a SnO<sub>2</sub>/Ag/SnO<sub>2</sub> structure including index matching layer were investigated. For the index matching materials, SiO<sub>2</sub> ( $n = 1.46$ ) and Nb<sub>2</sub>O<sub>5</sub> ( $n = 2.34$ ) were selected due to their low and high refractive index as well as outstanding thermal stability. The present research systematically evaluates the optical characteristics of a SnO<sub>2</sub>/Ag/Nb<sub>2</sub>O<sub>5</sub>/SnO<sub>2</sub> multilayer film with a varying thickness of the SnO<sub>2</sub> top layer. The optical characteristics are investigated, and the experimental results are compared to those obtained with the simulation program named EMP (essential macleod program).

### Experimental Details

#### Simulation

Prior to the experiments, the EMP was used to simulate the optical characteristics including the transmittance, reflectance and color in the multi-layer thin films. The EMP was performed through the following steps. First, the construction parameters such as the reflectance and extinction coefficient of SnO<sub>2</sub>, Ag, Nb<sub>2</sub>O<sub>5</sub>, SiO<sub>2</sub> and

\*Corresponding author:  
Tel : +82-43-261-2412,  
Fax: +82-43-271-3222  
E-mail: gejang@chungbuk.ac.kr

SnO<sub>2</sub> were calculated via ellipsometry measurements and were placed in the program. Second, the SnO<sub>2</sub>/Ag/Nb<sub>2</sub>O<sub>5</sub>/SiO<sub>2</sub>/SnO<sub>2</sub> multi-layered structures were designed and simulated using various parameters such as the wavelength ranges (380 ~ 780 nm), thickness (10 ~ 55 nm) and layers of the structure. Finally, an analysis of the parameter effect was performed with a system modification for the optical properties whether it is appropriate for the optimum simulation.

### Film preparation

For the purpose of this study, an SnO<sub>2</sub> (40 ~ 55 nm)/Ag (10 nm)/Nb<sub>2</sub>O<sub>5</sub> (10 nm)/SiO<sub>2</sub> (10 nm)/SnO<sub>2</sub> (25 nm) multi layered film with more than about 85% transmittance was selected after taking a number of simulations by modifying the stacking sequence and by adjusting the thickness of each layer. Fig. 1 shows a schematic diagram illustrating the structure of the SnO<sub>2</sub>/Ag/Nb<sub>2</sub>O<sub>5</sub>/SiO<sub>2</sub>/SnO<sub>2</sub> multilayer film. A hybrid structure consisting of SnO<sub>2</sub>/Ag/Nb<sub>2</sub>O<sub>5</sub>/SiO<sub>2</sub>/SnO<sub>2</sub> was deposited on the soda lime glass substrate via sequential RF/DC magnetron sputtering at room temperature. Prior to deposition, the soda-lime glass substrate (75 × 25 × 1 mm<sup>3</sup>) was ultrasonically cleaned in acetone, ethanol and IPA for 30 min at 50 °C. Thin film layers of SnO<sub>2</sub>, SiO<sub>2</sub>, and Nb<sub>2</sub>O<sub>5</sub> were deposited via RF magnetron sputtering onto soda-lime glass substrates at room temperature. High purity Ar (35 sccm) was introduced into the chamber by using a mass flow meter with a total pressure at 5.5 mTorr. An Ag layer was deposited via DC magnetron sputtering, and the total film thickness was of about 100 nm. The thickness of each layer was controlled through an increase in the sputtering time at constant optimized conditions. The refractive index *n* and the extinction coefficient *k* of each monolayer were evaluated using an ellipsometer (Elli-SE) in the visible range from 350 to 750 nm with a step width of 5 nm. The micro-structural examination and surface roughness of the films was investigated via field emission electron

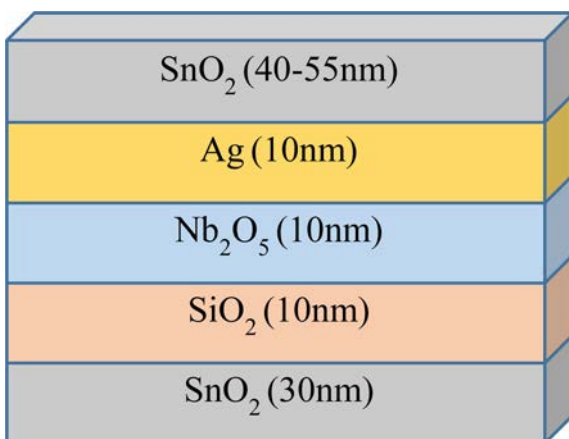


**Fig. 1.** A schematic diagram illustrating the structure of the SnO<sub>2</sub>/Ag/Nb<sub>2</sub>O<sub>5</sub>/SiO<sub>2</sub>/SnO<sub>2</sub> multi layer film.

microscopy (LEO-1530) and atomic force microscopy (AFM) in the contact mode. The transmittance and reflectance of the films were estimated using a UV-VIS-NIR spectrophotometer (Konika-Minolta CM-3600d) with a light source of D65. In addition, the interfacial properties of the SnO<sub>2</sub>/Ag/Nb<sub>2</sub>O<sub>5</sub>/SiO<sub>2</sub>/SnO<sub>2</sub> electrodes were analyzed using AES depth profiling. The sheet resistance was then detected using a four-point probe system.

## Results and Discussion

### Optical Properties

The refractive index *n* and extinction coefficient *k* are necessary to obtain an accurate analysis from the EMP simulation. Fig. 2 represents the measured refractive index *n* and the extinction coefficient *k* for SiO<sub>2</sub>, Nb<sub>2</sub>O<sub>5</sub>, SnO<sub>2</sub> and the Ag thin film in the visible range, as evaluated by the ellipsometry measurements using an ellipsometer (Elli-SE). The refractive indexes obtained for the SiO<sub>2</sub>, Nb<sub>2</sub>O<sub>5</sub>, SnO<sub>2</sub> and Ag thin films were of 1.52, 2.42, 2.09 and 0.12, respectively, which are somewhat higher than that of a theoretical value. The slightly high value of *n* is thought to rise from the low density and low crystallinity of each film due to their low processing temperature. Furthermore, the extinction coefficients measured for SiO<sub>2</sub>, Nb<sub>2</sub>O<sub>5</sub>, SnO<sub>2</sub> and Ag are 0.02, 0.0, 0.0 and 2.98, respectively. Table 1 shows a comparison of the refractive index *n* and the extinction coefficient *k* with theoretical and experimental data, respectively.

Prior to the experiments, the EMP was carried out to simulate the optical characteristics. The results of the simulations indicated that the film thickness of the top

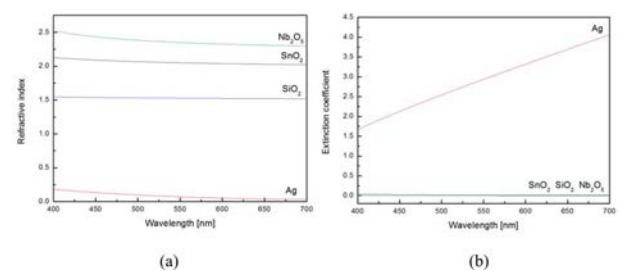


**Fig. 2.** (a) The measured refractive index *n* and (b) extinction coefficient *k* for SiO<sub>2</sub>, Nb<sub>2</sub>O<sub>5</sub>, SnO<sub>2</sub> and Ag thin film in visible range.

**Table 1.** Comparison of the refractive index *n* and extinction coefficient *k* with theoretical and experimental data.

Materials	Theoretical value		Experimental value	
	<i>n</i>	<i>k</i>	<i>N</i>	<i>k</i>
SnO <sub>2</sub>	1.46	0	1.52	0.02
Nb <sub>2</sub> O <sub>5</sub>	2.34	0	2.42	0
SnO <sub>2</sub>	2.04	0	2.09	0
Ag	0.15	3.47	0.12	2.98

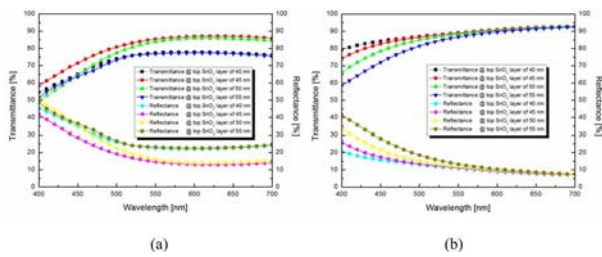


**Fig. 3.** (a) Simulated and (b) experimentally-measured optical characteristics on SnO<sub>2</sub>/Ag/Nb<sub>2</sub>O<sub>5</sub>/SiO<sub>2</sub>/SnO<sub>2</sub> multi layer film as a function of thickness of the top SnO<sub>2</sub> layer.

SnO<sub>2</sub> layer varied from 40 to 55 nm, the SiO<sub>2</sub>, Nb<sub>2</sub>O<sub>5</sub> and Ag layers were fixed at 10 nm, and the bottom SnO<sub>2</sub> layer remained at 30 nm. Fig. 3(a) exhibited the optical simulation spectra of the transmittance on SnO<sub>2</sub> (40 ~ 55 nm)/Ag (10 nm)/Nb<sub>2</sub>O<sub>5</sub> (10 nm)/SiO<sub>2</sub> (10 nm)/SnO<sub>2</sub> (30 nm) multi layer film as a function of the top layer of SnO<sub>2</sub> thickness. As can be seen from the simulation spectra in Fig. 3(a), the transmittance gradually decreased from 89.0% to 86.7% at a 550 nm wavelength and the top SnO<sub>2</sub> thickness increased from 40 to 55 nm. Also, the reflectance of multi-layer films gradually increased from 10.9% to 13.3% as a function of top SnO<sub>2</sub> thickness. Fig. 3(b) shows the experimentally measured transmittance taken from the same multilayer films as a function of the top SnO<sub>2</sub> thickness. However, when compared to that obtained through a simulation, the transparencies obtained from the experimental spectra dramatically increased from 77.4% to 85.3% at 550 nm wavelength, and the transmittance gradually decreased, relatively. The reflectance also decreased from 22.4% for 40 nm top SnO<sub>2</sub> layer to 14.1% for 45 nm top SnO<sub>2</sub> layer at 550 nm wavelength; a similar trend has been exhibited for transmittance spectra. This

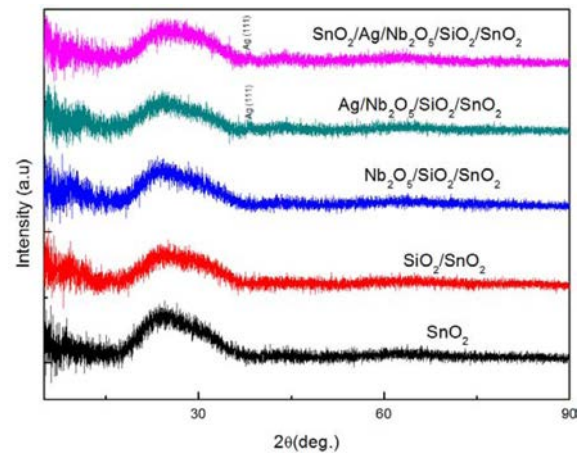


**Fig. 4.** XRD patterns obtained from SnO<sub>2</sub> (45 nm)/Ag (10 nm)/Nb<sub>2</sub>O<sub>5</sub> (10 nm)/SiO<sub>2</sub> (10 nm)/SnO<sub>2</sub> (30 nm) multi layer film with stacking process.

might be attributed to light scattering on each layer of the film surface and the interface instability due to the elemental diffusion. Moreover, the substrate temperature was also considered to cause a difference in the crystallinity of each layer between the experimental and the EMP simulation results.

#### Phase identification and surface morphology analysis

Fig. 4 presents the XRD patterns obtained from SnO<sub>2</sub> (45 nm)/Ag (10 nm)/Nb<sub>2</sub>O<sub>5</sub> (10 nm)/SiO<sub>2</sub> (10 nm)/SnO<sub>2</sub> (30 nm) multi layer film with stacking process. As can be seen in Fig. 4, all as-deposited films appear to be amorphous during the deposition process. The broad diffraction peak at 26° for all samples is caused by the glass substrate, which can be explained by the thin film with about 100 nm thick having a nanocrystalline phase,

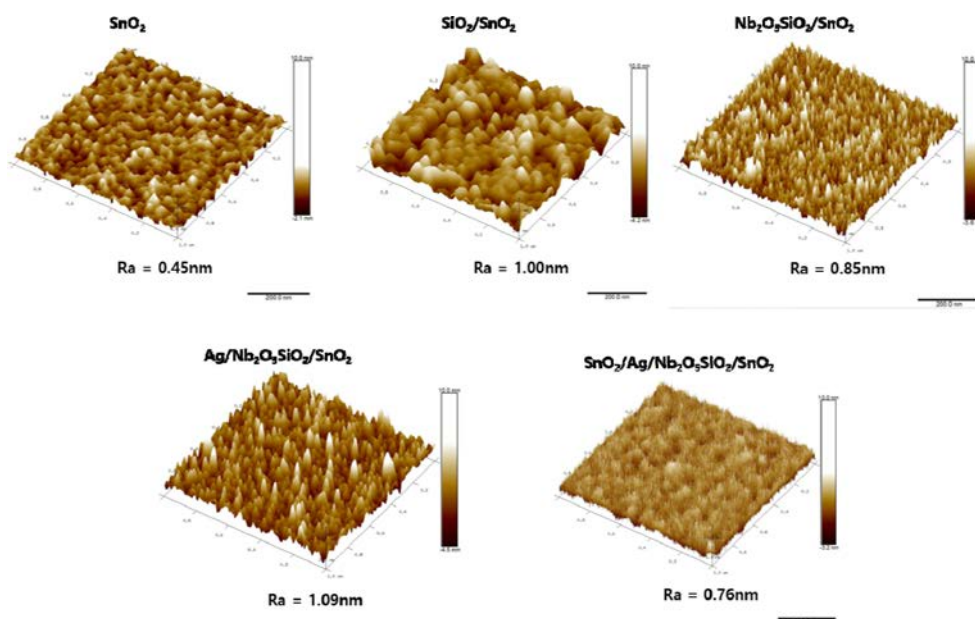


**Fig. 5.** The change in surface roughness of the SnO<sub>2</sub>/Ag/Nb<sub>2</sub>O<sub>5</sub>/SiO<sub>2</sub>/SnO<sub>2</sub> multilayer films with stacking process.

formed during the DC/RF sputtering process. Also one prominent peak of Ag (111) at around  $38.2^\circ$  was observed after the deposition of Ag on  $\text{SnO}_2/\text{SiO}_2/\text{Nb}_2\text{O}_5$  multi layer film. Fig. 5 shows the AFM images of  $\text{SnO}_2$  (45 nm)/Ag (10 nm)/ $\text{Nb}_2\text{O}_5$  (10 nm)/ $\text{SiO}_2$  (10 nm)/ $\text{SnO}_2$  (30 nm) multilayer film. While the film deposition was performed, the surface roughnesses are very smooth and remained relatively small below the 2 nm.

### Electrical properties analysis

The variation in the sheet resistance ( $R_s$ ) and resistivity ( $\rho$ ) of the coated multi layers as a function of the  $\text{SnO}_2$  layer thickness are displayed in Fig. 6. The resistance measured for the multi layers,  $R_s$ , can be defined as a function of the resistance of the single layers coupled in parallel, as described in the following equation [18]:

$$\frac{1}{R_s} = \frac{1}{R_{\text{SnO}_2\text{bot}}} + \frac{1}{R_{\text{Ag}}} + \frac{1}{R_{\text{Nb}_2\text{O}_5}} + \frac{1}{R_{\text{SiO}_2}} + \frac{1}{R_{\text{SnO}_2\text{top}}} \quad (1)$$

Where  $R_s$  is the sheet resistance of the multi layers,

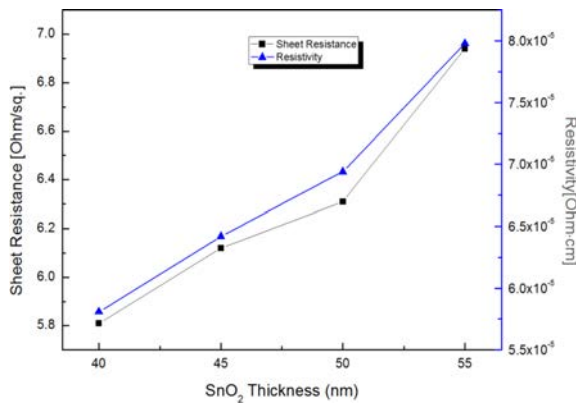


**Fig. 6.** Variation in the sheet resistance ( $R_s$ ) and resistivity ( $\rho$ ) of  $\text{SnO}_2/\text{Ag}/\text{Nb}_2\text{O}_5/\text{SiO}_2/\text{SnO}_2$  coated multi layer as a function of top  $\text{SnO}_2$  layer thickness.

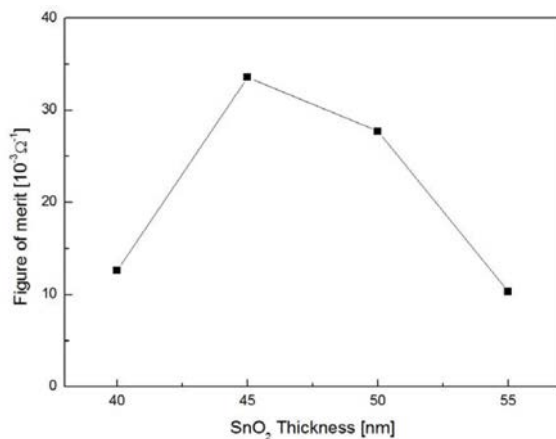


**Fig. 7.** The calculated  $\Phi_{\text{TC}}$  with an increase in the top  $\text{SnO}_2$  layers in  $\text{SnO}_2/\text{Ag}/\text{Nb}_2\text{O}_5/\text{SiO}_2/\text{SnO}_2$  multi layer film.

$R_{\text{SnO}_2\text{top}}$ ,  $R_{\text{Ag}}$ ,  $R_{\text{Nb}_2\text{O}_5}$  and  $R_{\text{SnO}_2\text{bot}}$  are the sheet resistance of the top  $\text{SnO}_2$ , Ag,  $\text{Nb}_2\text{O}_5$  and the bottom  $\text{SnO}_2$ , respectively.

From Fig. 6, the lowest  $R_s$  and  $\rho$  value were of about  $5.81 \Omega/\text{sq}$  and  $5.81 \times 10^{-5} \Omega \cdot \text{cm}$ , which were obtained with the multi-layer structure consisting of  $\text{SnO}_2$  (40 nm)/Ag (10 nm)/ $\text{Nb}_2\text{O}_5$  (10 nm)/ $\text{SiO}_2$  (10 nm)/ $\text{SnO}_2$  (30 nm). Moreover, the sheet resistance and resistivity of the  $\text{SnO}_2/\text{Ag}/\text{Nb}_2\text{O}_5/\text{SiO}_2/\text{SnO}_2$  multi layer films increased systematically with an increase in the thickness of the top  $\text{SnO}_2$  layer from 40 to 55 nm. In general, the total resistivity of the trilayer is determined mainly by the Ag layer [8]. However, in this study, the sheet resistance varied as a function of the top  $\text{SnO}_2$  layer thickness. In TCO applications, an optimization of the coating parameter plays a key role on the electric and optical characteristics. The figure of merit ( $\Phi_{\text{TC}}$ ), as derived by Haacke [19], is an important factor that represents the relationships between the sheet resistance and optical transmittance.

Fig. 7 demonstrated the  $\Phi_{\text{TC}}$  calculated with an increase in the top  $\text{SnO}_2$  layer. The  $\Phi_{\text{TC}}$  value of the  $\text{SnO}_2/\text{Ag}/\text{Nb}_2\text{O}_5/\text{SiO}_2/\text{SnO}_2$  multi layer film was shown to be in the range from  $10.35 \sim 33.6 \times 10^{-3} \Omega^{-1}$ . The  $\text{SnO}_2/\text{Ag}/\text{Nb}_2\text{O}_5/\text{SiO}_2/\text{SnO}_2$  multi layer with a 55 nm  $\text{SnO}_2$  thickness resulted in a decrease in  $\Phi_{\text{TC}}$  due to the decrease in transmittance. The highest  $\Phi_{\text{TC}}$  value ( $33.6 \times 10^{-3} \Omega^{-1}$ ) for the  $\text{SnO}_2/\text{Ag}/\text{Nb}_2\text{O}_5/\text{SiO}_2/\text{SnO}_2$  film was obtained at the top  $\text{SnO}_2$  thickness of 45 nm.

### Conclusions

In summary, this study systematically investigated the characteristics of RF/DC sputtering grown hybrid films with a structure consisting of  $\text{SnO}_2/\text{Ag}/\text{Nb}_2\text{O}_5/\text{SiO}_2/\text{SnO}_2$  with a varying  $\text{SnO}_2$  thickness. EMP was adopted to estimate the optical characteristics, and the refractive index  $n$  and extinction coefficient  $k$  were measured to make a comparison with experimental results. The transmittances were dependent on the  $\text{SnO}_2$  thickness. The measured transmittance suggested that a multilayered thin film of  $\text{SnO}_2$  (45 nm)/Ag (10 nm)/ $\text{Nb}_2\text{O}_5$  (10 nm)/ $\text{SiO}_2$  (10 nm)/ $\text{SnO}_2$  (30 nm) exhibited a high transmittance of 85.3 % at 550 nm. The XRD patterns obtained from the  $\text{SnO}_2$  (45 nm)/Ag (10 nm)/ $\text{Nb}_2\text{O}_5$  (10 nm)/ $\text{SiO}_2$  (10 nm)/ $\text{SnO}_2$  (30 nm) multi layer film appear to be amorphous because the fabrication of films was prepared at room temperature. The lowest  $R_s$  and  $\rho$  value were about  $5.81 \Omega/\text{sq}$  and  $5.81 \times 10^{-5} \Omega \cdot \text{cm}$ , acquired with the multi-layered film with a structure of  $\text{SnO}_2$  (40 nm)/Ag (10 nm)/ $\text{Nb}_2\text{O}_5$  (10 nm)/ $\text{SiO}_2$  (10 nm)/ $\text{SnO}_2$  (30 nm). However, the sheet resistance and resistivity of the  $\text{SnO}_2/\text{Ag}/\text{Nb}_2\text{O}_5/\text{SiO}_2/\text{SnO}_2$  multi layer films increased systematically with an increase in the thickness of the top  $\text{SnO}_2$  layer from 40 to 55 nm. The  $\text{SnO}_2/\text{Ag}/\text{Nb}_2\text{O}_5/\text{SiO}_2/\text{SnO}_2$  multi layer with 55 nm of  $\text{SnO}_2$  thickness resulted in a

decrease in  $\Phi_{TC}$  due to the decrease in transmittance. The highest  $\Phi_{TC}$  value ( $33.5 \times 10^{-3} \Omega^{-1}$ ) of the SnO<sub>2</sub>/Ag/Nb<sub>2</sub>O<sub>5</sub>/SiO<sub>2</sub>/SnO<sub>2</sub> film was obtained at the top SnO<sub>2</sub> thickness of 45 nm.

### Acknowledgments

This work was supported by the Industrial Technology Innovation Program, funded by the Ministry of Trade, Industry and Energy (MOTIE, Korea) (No. 10040000-10048659).

### References

1. V. Sharma, S. Singh, K. Asokan, K. Sachdev, Nuclear Instruments and Methods Research B 379 (2016) 141-145.
2. S. Hamrit, K. Djessas, N. Brihi, B. Viallet, K. Medjnoun, S.E. Grillo, Ceramics International 42 (2016) 16212-16219.
3. M. Chalh, S. Vedraïne, B. Lucas, B. Ratier, Solar Energy Materials & Solar Cells 152 (2016) 34-41.
4. Z. Xiao, J. Elike, A. Reynolds, R. Moten, X. Zhao, Microelectronic Engineering 164 (2016) 123-127.
5. X. Li, L. Colombo, R.S. Ruoff, Advanced Materials 28 (2016) 6247-6252.
6. B. Sciacca, J. Groep, A. Polman, E.C. Garnett, Advanced Materials 28 (2016) 905-909.
7. F. Dautou, P. C. P. Bouten, A. Dabirian, Y. Letierrier, C. Ballif, M. Morales-Masis, Organic Electronics 35 (2016) 136-141.
8. A.T. Barrows, R. Masters, A.J. Pearson, C. Rodenburg, D.G. Lidzey, Solar Energy Materials & Solar Cells 144 (2016) 600-607.
9. J.L. Yu, S.Y. Lee, Transactions on Electrical and Electronic Materials 17 [4] (2016) 201-203.
10. S.H. Park, S.J. Lee, J.H. Lee, J. Kal, J. Hahn, H.K. Kim, Organic Electronics 30 (2016) 112-121.
11. M. Kim, C. Lim, D. Jeong, H.S. Nam, J. Kim, J. Lee, Organic Electronics 36 (2016) 61-67.
12. C.H. Lee, R. Pandey, B.Y. Wang, W.K. Choi, D.K. Choi, Y.J. Oh, Solar Energy Materials & Solar Cells 132 (2015) 80-85.
13. D. Miao, S. Jiang, S. Shang, Z. Chen, Ceramics International 40 [8] (2014) 12847-12853.
14. J.G. Kim, S.M. Yoon, G.E. Jang, Journal of Ceramic Processing Research 17 [2] (2016) 80-84.
15. S. Li, Y. Dan, J. Zhou, H. Shen, Thin Solid Films 615 (2016) 56-62.
16. C. Tung, E. Dorjgotov M. Kuwabara, S. Kang, C. Chen, J.Z. Zhong, US Patent Application 20150316689 A1 (2015).
17. L. Huang, S.C. Chang, N. Oldham, S.P. Hotelling, J.Z. Zhong, C.H. Tung, US Patent Application 20100141608 A1 (2010).
18. S. Venkatachalam, H. Nanjo, K. Kawasaki, Y. Wakui, H. Hayashi, T. Ebina, Applied Surface Science 257 [21] (2011) 8923-8928.
19. G. Haacke, Journal of Applied physics 47 (1976) 4086-4089.